

PAPER

# Experiment demonstration of backward-propagating surface plasmon resonance mode

To cite this article: Yuying Tong *et al* 2017 *J. Opt.* **19** 124001

View the [article online](#) for updates and enhancements.

# Experiment demonstration of backward-propagating surface plasmon resonance mode

Yuying Tong<sup>1,2</sup>, Hailang Dai<sup>1,2</sup> and Xianfeng Chen<sup>1,2</sup> 

<sup>1</sup>The State Key Laboratory on Fiber Optic Local Area Communication Networks and Advanced Optical Communication Systems, School of Physics and Astronomy, Shanghai Jiao Tong University, Shanghai 200240, People's Republic of China

<sup>2</sup>Collaborative Innovation Center of IFSA (CICIFSA), Shanghai Jiao Tong University, Shanghai 200240, People's Republic of China

E-mail: [xfchen@sjtu.edu.cn](mailto:xfchen@sjtu.edu.cn)

Received 12 September 2017

Accepted for publication 6 October 2017

Published 26 October 2017



CrossMark

## Abstract

Surface plasmon resonance (SPR) is the physical process of surface plasmon excitation. The polarization sensitivity of the coupling efficiency and control of the directionality of SPR are facing challenges. We have experimentally demonstrated a new plasmonic coupler that overcomes these challenges using nano scale particles on a silver film. Our device is based on the Mie scattering of SPR and achieves a complete bidirectional excitation. The proposed design can be used to create sensors with both bidirectional and unidirectional launching of SPR, and consequently, can be extended to a broad range of applications in biosensor systems.

Keywords: surface plasmon resonance, Mie scattering, bidirectional excitation

(Some figures may appear in colour only in the online journal)

## 1. Introduction

Surface plasmon wave (SPW) is a surface electromagnetic wave that propagates at the boundary between a dielectric and a metallic medium. Since Wood's initial discovery of surface plasmon resonance (SPR) phenomenon in optical experiments in 1902 [1], it has been extensively studied and has gained an increased prominence. The wave vector of the SPW is larger than that of the free-space wave. Therefore in order to excite a SPW from a free-space illuminating beam, an additional contribution of momentum is required. Several methods have been proposed to realize SPR. The grating structure can be used to compensate for the wave vector mismatch at the boundary and excite the SPW [2]. Kretschmann and Otto have demonstrated the optical excitation of surface plasmons through attenuated total reflection (ATR) [3, 4].

In addition to the fundamental research, diverse techniques utilizing the optical characteristics of SPR have also been developed. SPR has been widely used in chemical, and, especially biological sensing [5–8]. One of the advantages of SPR is the ability to perform real-time analysis of biospecific

interactions with label-free molecules. SPR has been used in environmental monitoring, medicine, and food analysis, among others. Owing to a strong localization property of the electromagnetic field, it is possible to further extend the detection limit of this method [9]. Other applications of SPR also have been investigated, such as SPR interferometry [10, 11], SPR fluorescence spectroscopy [12, 13], SPR microscopy [14, 15], and nanosized particle characterization [16], among others.

In this study, we have demonstrated an occurrence of a backward light arc when the resonance condition of SPR was satisfied. This phenomenon is associated with the backward-propagating SPR mode. Several experiments were done to verify the cause of this phenomenon. Careful analysis of the experimental results confirmed that this phenomenon was caused by the Mie scattering of the SPW. Moreover, the uneven intensity distribution of the two light arcs observed in the experiment was caused by the uneven intensity distribution of the Mie scattering. Using our proposed scheme, bidirectional SPWs can be directly and concurrently monitored.

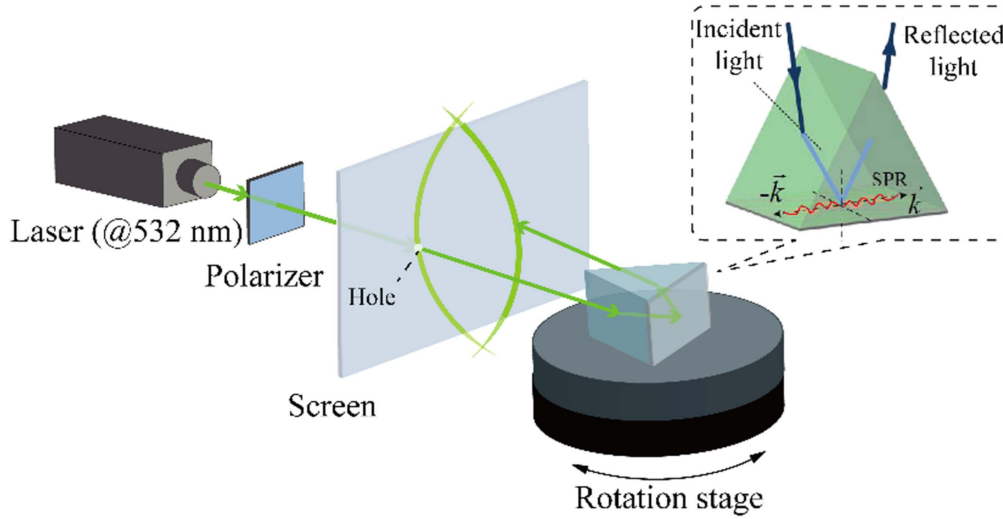


**Figure 1.** Schematic of the setup. The laser beam at 532 nm passes through a polarizer and through a hole in the screen. The laser beam then impinges on a prism, which is placed on a rotation stage, and is reflected by the prism/metal interface. The reflected light is projected on the screen.

## 2. Theoretical analysis

The transverse magnetic (TM) polarized light makes total reflection at the boundary between a glass and a metallic film. The resonance takes place when the horizontal component of the wave vector of incident light is equal to the wave vector of the surface plasmons. Under such resonance condition, the incident angle is defined as the resonance angle, and the resonance condition can be written as

$$k_0 n_p \sin \theta = k_0 \sqrt{\frac{\varepsilon_r n_a^2}{\varepsilon_r + n_a^2}}, \quad (1)$$

where  $k_0$  is the wave vector of incident light,  $n_p$  is the refractive index of a prism,  $\theta$  is the incident angle on the prism/metal interface,  $\varepsilon_r$  is the real part of the dielectric constant of the metal, and  $n_a$  is the refractive index of the object to be measured. In our experiment,  $n_a$  is the refractive index of air.

The relationship between reflectivity  $R$  and the incident angle  $\theta$  can be given by [17]:

$$R = \left| \frac{B}{A} \right|^2 = \left| \frac{\gamma_{12} + \gamma_{01} e^{-2\alpha_1 d}}{1 + \gamma_{12} \gamma_{01} e^{-2\alpha_1 d}} \right|^2, \quad (2)$$

where  $A$  is the intensity of the incident light and  $B$  is the intensity of the reflected light.  $\gamma_{01} = \frac{\varepsilon_0 \alpha_1 - \varepsilon_1 \alpha_0}{\varepsilon_0 \alpha_1 + \varepsilon_1 \alpha_0}$ ,  $\gamma_{12} = \frac{\varepsilon_1 \alpha_2 - \varepsilon_2 \alpha_1}{\varepsilon_1 \alpha_2 + \varepsilon_2 \alpha_1}$ .  $\alpha_j = (\beta^2 - k_0^2 \varepsilon_j)^{1/2}$  ( $j = 0, 1, 2$ ) are the attenuation coefficients,  $\beta = k_0 \sqrt{\varepsilon_2} \sin \theta$  is the propagation constant of the horizontal component of the wave vector. The dielectric constants of the prism and the air are  $\varepsilon_2$  and  $\varepsilon_0$ , respectively. The SPW propagates along the metal/air interface.

## 3. Methods

The schematic of the experimental setup is shown in figure 1. This experiment utilized a continuous-wave laser with a wavelength of 532 nm. The polarizer was used to control the polarization of the incident light (TM polarized) to ensure the excitation of SPR. The laser beam passed through the polarizer and through a hole in the screen. The laser beam then impinged on a prism that was placed on a rotation stage in order to tune the incident angle. The incident light was reflected by the prism/metal interface. The reflected beam was projected on the screen in the far-field and was registered by a detector. An equilateral triangular prism ( $\varepsilon = 3.24$ ) was coated with a layer of silver film, which was sputter-deposited in vacuum (SPF-210B, Anelva Corporation) and had a dielectric constant of  $\varepsilon_{Ag} = -15.8 + 1.06i$ .

## 4. Results and discussions

In our experiment, the thickness of the silver film was about 80 nm, as shown in figure 2(a). First, when the resonance condition of SPR satisfies equation (1), the incident angle is equal to the resonant angle, and the two light arcs are observed (see figure 2(b)). The A and B spots are the incident and emergent spots of the light, respectively. They are located in the left (spot A) and right (spot B) light arcs. The reflectivity at the reflection-point is measured with respect to the incident angle, as shown in figure 2(c) (theoretical calculation is obtained from equation (2)). Second, the reflectivity of the backward propagating light is also measured with respect to the incident angle, as shown in figure 2(d). Comparing the forward and backward ATR curves, as shown in figures 2(c) and (d), we see that the ATR angle is almost the same ( $30.7^\circ$ ). However, because of the beam intensity losses, the backward SPW is larger than the forward SPW and has a wider full width at half maximum (FWHM). In addition to the forward

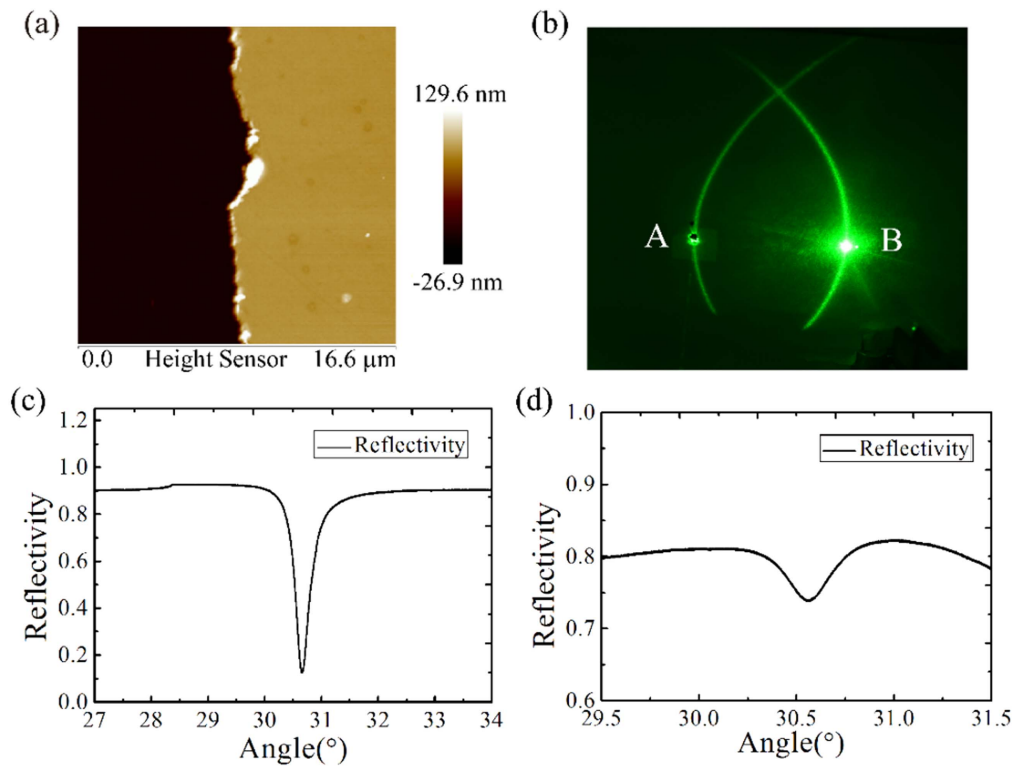


**Figure 2.** (a) AFM image of the silver film. (b) Two light arcs obtained in the experiment. (c) Experimental forward ATR curve. (d) Experimental backward ATR curve.

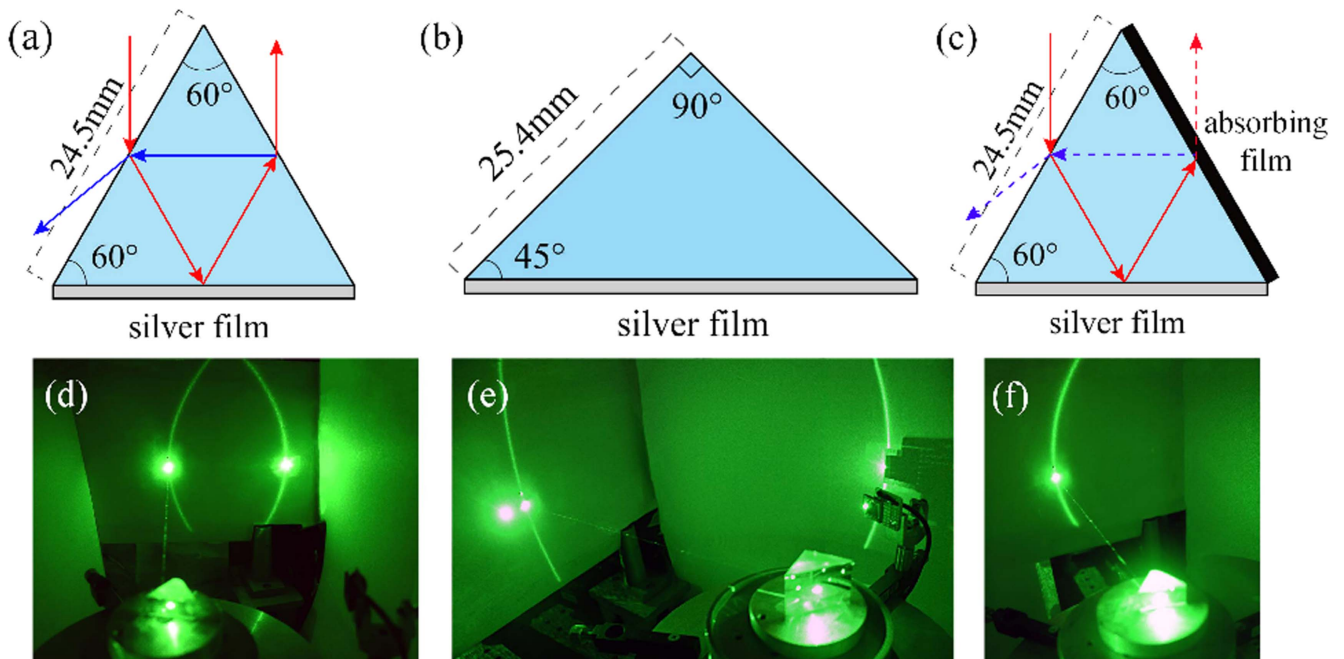


**Figure 3.** (a)–(c) Prisms used in the experiment. The prism in (c) is coated with an absorbing film so that the reflected light can be extinguished. (d)–(f) Experimental results of (a)–(c), respectively.

and backward directions, the SPW is also excited in other directions, resulting in longer light arcs. In the experiment, we observed that the right light arc being brighter than the left light arc.

There are four possible ways to explain the observation of the forward and backward SPWs. They could be due to the secondary reflections at the exit facet of the prism, the scattering of incident light, the excited light generated by

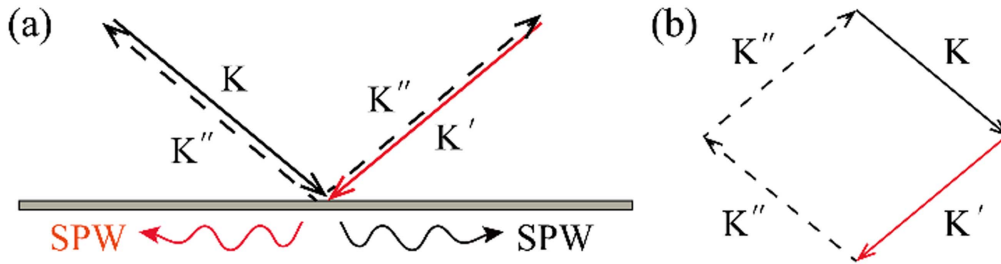


**Figure 4.** (a) The process of backward SPR same as that of forward SPR. (b)  $K'$  is produced by DFWM.

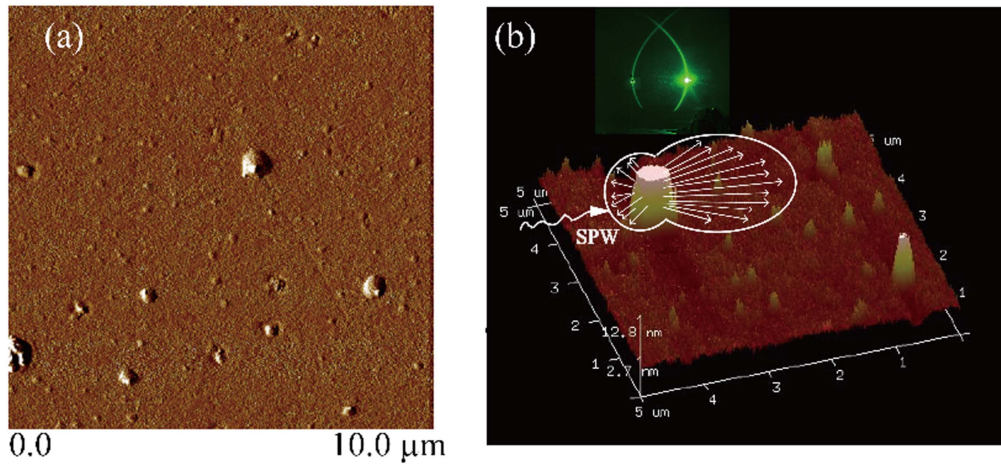


**Figure 5.** (a) AFM image of the silver film (2D). (b) AFM image of the silver film (3D); SPW is scattered by the silver particles that are larger than the wavelength of the incident light. There are two bright arcs on the screen.

degenerate four-wave mixing (DFWM) or due to the scattering of SPW.

First, prisms with different top angles ( $60^\circ$  and  $90^\circ$ ) were used in the experiment, as illustrated in figures 3(a) and (b). The side length of the equilateral prism in figure 3(a) is 24.5 mm and the hypotenuse of the right-angle prism in figure 3(b) is 25.9 mm. The corresponding experimental results are shown in figures 3(d) and (e), respectively. We can see that the reflection points in both of these cases were located on the left light arc. Next, an absorbing film was coated on the side of the prism that was the exit facet, as shown in figure 3(c). In this case, the reflected light is absorbed by the absorbing film and the right light arc disappeared, as shown in figures 3(c) and (f), while the left arc was still present. In all three cases, the positions of the left light arcs are unchanged with respect to the reflection spot. Hence, we can conclude that this phenomenon is not caused by the secondary reflections due to the prism.

Second, if the incident light falls on the metal particle, the scattered light could not reach the silver film in the form of an evanescent wave and, hence, SPR cannot be excited. On the other hand, when the incident light is coupled to the silver film, it will not be scattered. Moreover, if these two light arcs were caused by the scattering of the incident light, the scattered light would exhibit as the homogeneous property in all of the solid angle, so there will be faculae on the screen.

Third, if this phenomenon is also due to SPR, then it requires the incident light wave vector  $K'$  to come from a multi-wave coupling process, the DFWM.

The incident light with a wave vector  $K$  falls on the silver film and is scattered by it, so that the scattered lights with the same wave vector  $K''$  appear. According to DFWM, the light with wave vector  $K'$  is obtained when the momentum conservation condition is satisfied, as shown in figure 4. Moreover, in figure 2(b), we can see that the intensity of the left light arc is nearly 30% of the right light arc's intensity. However, in our experiment, because the incident light is a continuous light, the light with wave vector  $K'$  cannot have 30% of the efficiency. Therefore, the only possible cause of this phenomenon is due to the scattering of the SPW.

In order to confirming the above hypothesis, we analysed the topography of the silver film with the atomic force microscope (AFM). The obtained 2D and 3D images used in our experiment are shown in figures 5(a) and (b). We can see that the surface of the silver film is rough. The SPW will be excited when the resonance condition is satisfied. As this SPW propagates forward, it will be scattered by the particles present on the silver film. The measured surface roughness was about 700 nm, which is comparable to the wavelength of the incident light (532 nm). This is the size regime of the Mie scattering and its scattering intensity distribution is shown in figure 5(b). We note that the interaction of light with a rough metal surface has been studied previously [18–21]. In the work of Hunderi and Beaglehole [22], it can be described as the fact of the excitation and subsequent radiation of surface polaritons. They also used Mie's solution to calculate the scattering and extinction cross sections of the isolated spheres [22–24]. Additionally, Celli has studied the two problems



involving the interaction of a volume electromagnetic wave with a randomly rough metal surface [25]. In our experiment, the phenomenon satisfies the characteristics of Mie scattering in which the intensity of the forward scattered wave is stronger than that of the backscattering wave. Moreover, as the particle size increases, the intensity of the forward scattering also gradually increases while the backscattering intensity gradually decreases.

In principle, on the basis of the Mie scattering theory, the forward SPW and backward scattered SPW ought to be propagating in all of the directions along the silver film resulting in a complete ring pattern. However, in our experiment, only two light arcs are observed. The light that is perpendicular to the direction of the incident plane has almost completely disappeared. This phenomenon mainly comes from the weak scattering perpendicular to the direction of the incident light and the strong absorption of the silver film.

Because of the bidirectional SPR, the additional information carried by SPR process can be obtained by measuring the backward SPW. Comparing the forward ATR curve with the backward ATR curve enables us to determine the refractive index of the tested objects. From the Mie scattering, we can obtain the information about the density and size of the scatterer. If the scatterer is a liquid, its concentration may be determined.

## 5. Conclusion

In conclusion, two light arcs are observed in the experiment when the resonance condition of SPR is satisfied. A series of comparative experiments and theoretical analysis has been carried out to confirm the mechanism of this phenomenon. The cause was determined to be due to the Mie scattering of the SPW. Moreover, the uneven intensity distribution of two light arcs observed in the experiment correlates with the uneven intensity distribution of the Mie scattering. In our proposed scheme, bidirectional SPWs can be directly and concurrently monitored. This phenomenon may have potential applications in biological sensing and biological detection.

## Acknowledgments

National Natural Science Foundation of China (61235009), the National Basic Research Programmer of China (Grant No. 2013CBA01703).

## ORCID iDs

Xianfeng Chen  <https://orcid.org/0000-0003-3025-9729>

## References

- [1] Wood R W 1902 *Philos. Mag.* **18** 396–402
- [2] Alleyne C J, Kirk A G, McPhedran R C, Nicorovici N-A P and Maystre D 2007 *Opt. Express* **15** 8163–9
- [3] Kretschmann E 1971 *Z. Physik.* **241** 313–24
- [4] Otto A 1968 *Z. Physik.* **216** 398–410
- [5] Sun X C, Shiokawa S and Matsui Y 1989 *Japan. J. Appl. Phys.* **28** 1725–7
- [6] Salamon Z, Macleod H and Tollin G 1997 *Biochim. Biophys. Acta* **1331** 117–29
- [7] Wu C M and Pao M C 2004 *Opt. Express* **12** 3509–14
- [8] Karlsson R and Fält A 1997 *J. Immunol. Methods* **200** 121–33
- [9] Homola J 2008 *Chem. Rev.* **108** 462–93
- [10] Ho H and Lam W 2003 *Sensors Actuators B* **96** 554–9
- [11] Yu X L, Wang D X, Xing W, Ding X, Liao W and Zhao X S 2005 *Sensors Actuators B* **108** 765–71
- [12] Liebermann T, Knoll W, Sluka P and Herrmann R 2000 *Colloids Surf. A* **169** 337–50
- [13] Nenninger G G, Piliarik M and Homola J 2002 *Meas. Sci. Technol.* **13** 2038–46
- [14] Berger C E H, Kooyman R P H and Greve J 1994 *Rev. Sci. Instrum.* **65** 2829–36
- [15] Rothenhäusler B and Knoll W 1988 *Nature* **332** 615–7
- [16] Venkata P G, Aslan M M, Menguc M P and Videen G 2007 *J. Heat Transfer* **129** 60–70
- [17] Lopez-Rios T and Vuye G 1982 *J. Phys. E: Sci. Instrum.* **15** 456–61
- [18] West C S and O'Donnell K A 1996 *Opt. Commun.* **123** 109–14
- [19] Gersten J I, Weitz D A, Gramila T J and Genack A Z 1980 *Phys. Rev. B* **22** 4562–71
- [20] Schade H and Smith Z E 1985 *Appl. Opt.* **24** 3221–6
- [21] Zayats A V, Smolyaninov I I and Maradudin A A 2005 *Phys. Rep.* **408** 131–314
- [22] Hunderi O and Beaglehole D 1970 *Phys. Rev. B* **2** 321–9
- [23] Stern E A 1967 *Phys. Rev. Lett.* **19** 1321–4
- [24] Mie G 1908 *Ann. Phys.* **25** 377–445
- [25] Celli V, Maradudin A A, Marvin A M and McGurm A R 1985 *J. Opt. Soc. Am. A* **2** 2225–39